STATISTICAL ERROR STUDIES IN THE ESS LINAC

M. Eshraqi*, R. Miyamoto, E. Sargsyan, ESS, Lund, Sweden
R. De Prisco, ESS, Lund, Sweden and LNL-INFN, Legnaro, Italy
H. D. Thomsen, ISA, Aarhus, Denmark

Abstract

Following the completion of the latest layout of the ESS linac statistical error studies have been performed to define the field vector quality and alignment tolerances. Based on these tolerances and error study results a scheme for the correction system is proposed that assures low losses and permits hands-on maintenance. This paper reports on the strategy of simulating and performing the error studies as well as setting the tolerances.

INTRODUCTION

The high power linac of the European Spallation Source, ESS, accelerates 62.5 mA of protons up to 2 GeV in a sequence of normal conducting and superconducting accelerating structures. These protons are to be used for the spallation process in which a high flux of pulsed neutrons will be generated in a neutron rich target material.

The high reliability and availability of the accelerator requires short repair times which sets a loss limit for hands-on maintenance of the machine. Hands-on maintenance and machine protection set limits of 1 W/m and 0.1 W/dm respectively, on beam losses. On top of being demanding on the nominal design, the tolerances have to be studied as well to make sure that the accelerator, with realistic tolerances is capable of delivering 5 MW of power with power losses in the order of 10^{-7}. The 2013 baseline, code named OptimusPlus is presented in [1].

STRATEGY AND LIMITS

As the first step for starting the statistical error studies it is needed to define a strategy on how to proceed and where to set the limits or how large errors to accept. This process could be re-iterated as some of the resulted tolerances which are not very demanding could be tightened in favor of those which are more costly to achieve or maintain. For this first step, we have set the limits on losses at 99% confidence level to be within the 1 W/m limit. There is a limit on the emittance growth due to errors too. On the one hand not injecting into a ring ESS linac is not so restricted on the emittance of the final beam it delivers. On the other hand a significantly higher emittance could lead to major losses. Considering both arguments, an emtitance twice that of the nominal case without errors was set as the limit for the final emittance in the presence of errors.

ESS linac consists of 5 accelerating structures, RFQ, DTL, Spoke, medium-β, and high-β, plus two transport lines, MEBT, and HEBT. These sections have different lengths, but it takes almost the same time for the beam to travel

---

* mamad.eshraqi@esss.se

through each section. Therefore, the additional emittance growth per section due to errors was decided to be limited to $\sqrt[7]{2} - 1$, or 10% per section in each plane (for 99% of the cases), setting a second limit for defining tolerances.

Having set a strategy in place to define the static tolerances, it is also important to set the limit on dynamic errors and jitters. While the former is static and could be corrected or accounted for in the downstream structures or devices, the latter would be left uncorrected. To make sure the dynamic errors do not cause unwanted effects, the criteria to set them is to have an effect which is less than $1\times$ rms spread of the beam in the plane of study.

To study the transverse errors a functional beam trajectory correction system should be in place. This has been done by optimizing the positions of the steerers and their corresponding beam position monitors, BPMs, specially in the drift tube linac, DTL, where the number of choices is limited. The focus in the other parts of the linac has been on reducing the number of active BPMs, without loosing the control over beam trajectory. Enabling the correction system, with the right limit on the steerer strengths, the transverse tolerances have been set. These processes have been performed section by section and the tolerances for each section are set. To check the sensitivity to these errors, all the errors are applied at 50%, 100% and 150% of the accepted value. Finally, to investigate where the possible hot spots are and create a loss-map, errors are applied to the linac lattice from RFQ exit to the target.

Another type of errors, which has not yet been fully investigated is the systematic errors, such as floor settlement of the accelerator, phase reference line delays, or magnetic imperfections and multipoles.

ERRORS INVESTIGATED

The errors investigated in this study, irrespective of their time dependency belong to one of the following types: machining, welding, positioning, powering, and the input beam errors. The errors are uniformly distributed between plus and minus of the defined tolerance. These could be different from section to section.

RFQ

The beam is generated at the RFQ input, with a gaussian distribution truncated at $4 \times \sigma$ with 100,000 macroparticles [2]. To set the tolerances for acceptable beams, position, angle, and Twiss parameters of the beam have been varied. The machining errors in the RFQ include errors in the longitudinal and transverse profile of the vanes. Welding errors investigated are the vane welding errors that could be

vertical/horizontal shift of the vertical vanes (called parallel/perpendicular) in this study and the corresponding errors on horizontal vanes. These errors could have a different value, still within the limit, on two ends of the vane causing a tilt. The RFQ is being built in few sections, and the alignment of these units with respect to each other (shifts and tilts) are also included. The last error that has been covered in the RFQ is the voltage jitter. Tolerances of the RFQ are listed in table 1. The parameters of the beam, their average, and extents are saved at the end of the RFQ. The result of errors on the final beam out of the RFQ is presented in table 2.

Table 1: Tolerances of the ESS RFQ (Max Values)

Error	Value	Unit
Input beam alignment position	0.2	mm
Input beam alignment angle	2	mrad
Input beam Twiss mismatch (α)	20	%
Input beam Twiss mismatch (β)	10	%
Longitudinal vane profile	0.02	mm
Transverse vane curvature	0.02	mm
Parallel and perpendicular vane shift	0.03	mm
Parallel and perpendicular vane tilt	0.06	mrad
Horizontal and vertical segment shift	0.03	mm
Segment tilt around X and Y axis	0.06	mrad
Vane voltage jitter	0.5	%

MEBT, SCL, and HEBT

In the medium and high energy beam transport, MEBT and HEBT, and the superconducting linac (Spoke, medium-β and high-β sections), the errors applied are the following:
Quadrupoles: Alignment of the quadrupoles including their transverse position, rotations around the beam axis, and gradient errors. Rotation of quad perpendicular to the beam axis was excluded from these studies since the effect, under the same alignment condition, was negligible.
Cavities: Alignment of the cavities including their transverse position, rotations perpendicular to the beam axis, static and dynamic accelerating field amplitude and rf phase errors.
Dipoles: Alignment of the dipoles including their transverse position, rotations perpendicular to the beam axis, and field error.
Input beam: The variations of the beam parameters at the end of the RFQ with errors are used as beam errors at the input of the MEBT, including the position and angle errors, emittances, mismatch in Twiss parameters, energy jitter and current variations. The nominal distribution out of the RFQ is used as input distribution.

Table 2: Beam Errors Included in the Error Studies at the MEBT Input (Max Values)

| | dxy | dϕ | dxy' | dE | dϵ | m | dI |
	mm	deg	mrad	keV	%		mA
Beam	0.3	0	1	36.2	5	5	0.625

DTL

The DTL uses permanent magnet quadrupoles for transverse focusing [3]. Each tank is fed by one klystron and therefore all the errors caused at that level are coupled. Synchronous phase and field amplitude errors in each cell are determined by the shape and position of drift tubes and are uncoupled. The applied errors here are:
PMQs: The same types of errors as powered quadrupoles, with different amplitudes, are applied here.
RF: Uncoupled field and phase errors are applied to rf cells. These errors are due to machining or installation errors and are static in time. Coupled field and phase errors are applied to all cells of each tank. These errors are due to rf set points and are static and dynamic, with different amplitudes.

Table 3: Tolerances for the ESS Linac (Max Values)

| | Δ_{xy} | ϕ_{xy} | ϕ_z | ΔG | $\Delta\phi_{rf}$ | Δ_{rf} |
	mm	deg	deg	%	deg	%
			MEBT			
Quad	0.2		0.06	0.5		
Cav (S*)	0.5	0.115			1	1
Cav (D)					0.1	0.1
			DTL			
Quad	0.1	0.5	0.2	0.5		
Cell (S)					0.5	1
Tank (S)					1	1
Tank (D)					0.1	0.1
			SCL			
Quad	0.2		0.06	0.5		
Cav (S)	1.5	0.129			1	1
Cav (D)					0.1	0.1
			HEBT			
Quad	0.2		0.06	0.5		
Dipole	0.2		0.06	0.05		

* S: Static, D: Dynamic

ERROR STUDY

The error studies are performed using the code TraceWin [4], using 100,000 macro particles. The 3D PIC-NIC space charge routine is used with a $10 \times 10 \times 10$ mesh. The beam distribution at the beginning of RFQ is gaussian truncated at $4 \times \sigma$. The transported beam through the RFQ is saved and used for error studies. To define the dependencies on different parameters each parameter was studied individually (excluding the symmetries, e.g. between vertical and horizontal planes) in this stage. Each case is simulated using 1000 linacs with gradually increasing errors such that the aforementioned limits are not passed. Finally all the errors (including symmetries) are applied to each section to check if the combined effect of all errors is still within the limits. In the next stage the accelerator from RFQ exit to the target was used in the error studies. Tolerances of each component in each section is listed in table 3.

In the presence of these errors the beam behaves differently than nominal. The positions of the tracked particles are stored during error studies and post processing would show how close the beam gets to the aperture, and how much beam power is confined within a certain radius in the presence of errors. The power density levels which are indicators of these are shown in figure 1, and the average of the normalized rms emittances are shown in figure 2.
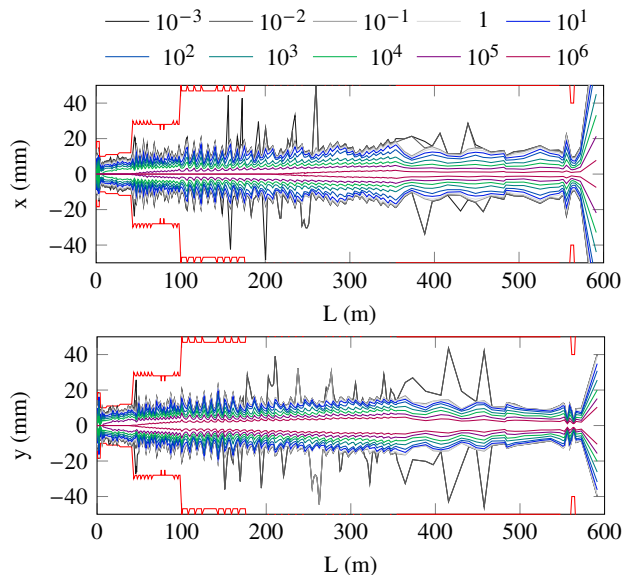

Figure 1: Power density levels from the RFQ exit to the target. The beam power outside of the outermost line is 1×10^{-3} W. Red line shows the beam aperture.
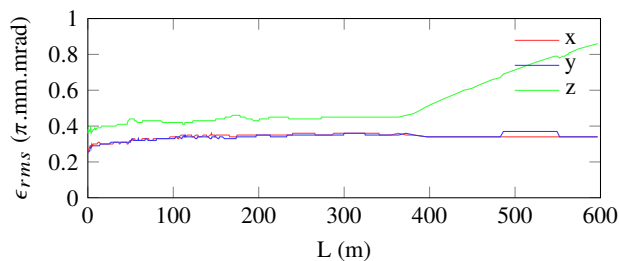

Figure 2: Average emittance evolution over 1000 linacs.

The average losses, mainly due to losses in longitudinal plane, and the confidence level of these losses are shown in figures 3 and 4. The peaks observed in these figures are due to the particles, which have not been captured inside the rf bucket after the frequency jump or have been in the tails of the beam out of the RFQ and are transported through the linac. These particles that are the cause of the increased halo observed in figure 1 are lost after the first vertical bend where off momentum particles are bent above the beam trajectory.

SUMMARY

The end to end runs have been performed using a gaussian beam truncated at $4 \times \sigma$, generated at the RFQ input. These beam has been transported through the RFQ and the output beam is used as the input distribution for the following
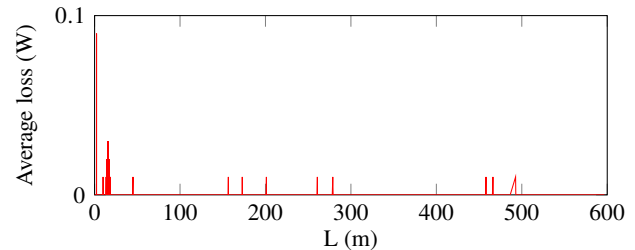

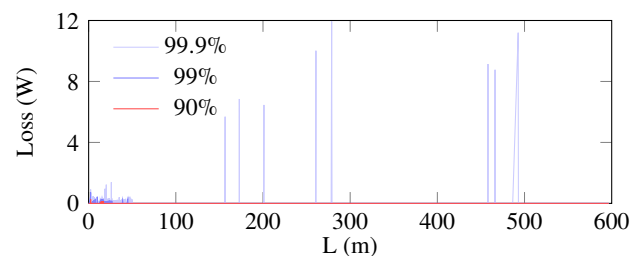Figure 3: Average beam power loss.

Figure 4: Confidence level beam power loss.

simulations and error studies. Individual error studies on stand-alone sections of the linac are performed to set the tolerances. To estimate the beam losses along the linac these tolerances are applied to an integrated lattice which runs from MEBT input to the HEBT output. These end to end error studies show that the average losses is in the order of 0.1 W, a number which is consistent with the losses observed at SNS with a proton beam. At 99% confidence level the beam power loss is less than 1 W in each meter.

REFERENCES

[1] M. Eshraqi, et.al. "The ESS Linac", *Proc. IPAC'14*, Dresden, Germany, THPME043.

[2] A. Ponton, "Note on the ESS RFQ Design Update", ESS Technical Report, 2014.

[3] R. D. Prisco, *et.al.*, "ESS DTL Status: Redesign and optimizations", *Proc IPAC'14*, Dresden, Germany, THPME041.

[4] R. Duperrier, N. Pichoff and D. Uriot, Proc. International Conf. on Computational Science, Amsterdam, The Netherlands, 2002.